

Evaluation of One-Dimensional Helical Coil Heat Exchanger Design Code (KAIST-HCHXD)

Yeongchan Kim^a, Jeong Ik Lee^{a*}

^aDept. Nuclear & Quantum Eng., KAIST, 373-1, Guseong-dong, Yuseong-gu, Daejeon, 305-701, Republic of Korea
*Corresponding author: jeongiklee@kaist.ac.kr

1. Introduction

With the development of small modular reactors (SMRs) and high-temperature gas-cooled reactors (HTGRs), helical coil heat exchangers have gained prominence due to their high thermal efficiency, compactness, and mechanical robustness. These heat exchangers have been utilized in systems such as advanced gas-cooled reactors (AGR) and liquid metal fast breeder reactors (LMFBR) and are being considered for high-temperature applications in the Next Generation Nuclear Plant (NGNP) program in the U.S [1, 2].

HTGRs, which use helium as a coolant, operate at much higher temperatures than traditional light water reactors (LWRs), making them suitable for process heat applications such as hydrogen production and industrial heat supply. To safely transfer thermal energy from the nuclear reactor to secondary systems, an intermediate heat exchanger (IHX) is required, ensuring system safety and operational flexibility.

The NGNP, designed for both electricity and hydrogen production, incorporates a helium-to-helium IHX capable of handling temperatures up to 1000°C. In Korea, similar efforts have been initiated for the development of high-temperature gas-cooled reactors aimed at process heat production.

This study evaluates the KAIST-developed one-dimensional Helical Coil Heat Exchanger Design Code (KAIST-HCHXD) by benchmarking it against IHX designs from General Atomics (GA) and AREVA [3,4]. While Argonne National Laboratory (ANL) has previously conducted similar studies [2], their specific methodology was not disclosed. In this study, the heat transfer and friction factor correlations used in ANL's work were applied, but the KAIST-HCHXD code was independently developed by KAIST. The research assesses the reliability and accuracy of KAIST-HCHXD in designing helical coil heat exchangers, demonstrating the consistency of the applied correlations within this design framework.

2. Methodology

2.1 Helical coil heat exchanger

A helical coil heat exchanger consists of tubes wound in a helical shape, allowing efficient heat transfer between two fluids. In this design, the secondary fluid flows inside the helical tubes, while the primary fluid passes over the coiled structure within a shell. As shown in Fig. 1., the key structural features of a helical coil heat

exchanger include helically wound tubes arranged in multiple layers to maximize heat transfer area. The tube pitch defines the spacing between adjacent coils, while the coil diameter determines the bending radius of the helical tubes. In the first layer, the coil diameter is the smallest, and as additional layers are added, the diameter increases according to the tube pitch length, resulting in a progressively larger helical structure. Additionally, the elevation angle (ϕ in Fig. 1) represents the inclination of the tubes relative to the horizontal axis, while the shell enclosure, which is an annular cylinder, houses the primary fluid as it flows across the coiled tubes. The total number of tubes increases as more layers are added, with the number of tubes per layer determined by the elevation angle. A larger elevation angle results in a greater increase in tube count between layers, while a smaller elevation angle leads to a more gradual increase. This relationship affects the overall heat exchanger design by influencing heat transfer capacity and flow distribution.

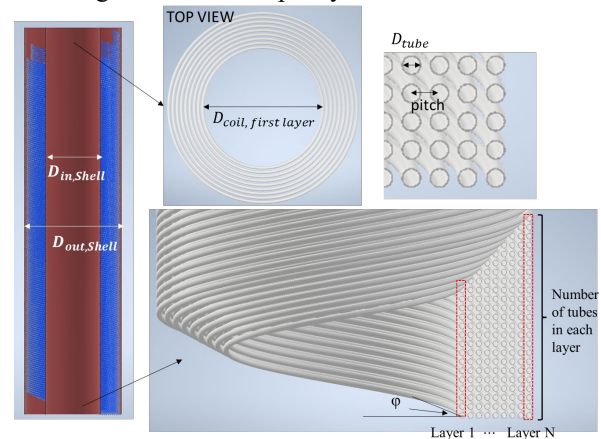


Fig. 1. Schematic representation of the helical coil heat exchanger geometry.

2.2 KAIST-HCHXD

This study utilizes the KAIST-developed one-dimensional Helical Coil Heat Exchanger Design Code (KAIST-HCHXD) to evaluate the thermal-hydraulic performance of a Helical Coil Heat Exchanger (HCHE). The code models heat transfer, pressure drop, and enthalpy variations for both the primary and secondary sides using a segmented approach. It iteratively solves temperature distributions, heat transfer coefficients, and pressure losses while ensuring convergence through dynamic length adjustments.

The code requires input data, including flow conditions (mass flow rate, temperature, pressure), geometric parameters (tube diameter, pitch, coil

diameter), and material properties. The secondary side is divided into multiple helical tube layers, and calculations proceed iteratively with convergence checks for wall temperature and outlet enthalpy. If convergence fails, the tube length is adjusted, and computations are repeated. The final output provides thermal-hydraulic design parameters, such as temperature profiles, heat transfer coefficients, and pressure drop, aiding in the design and optimization of helical type heat exchangers. The iteration logic is illustrated in Fig. 1.

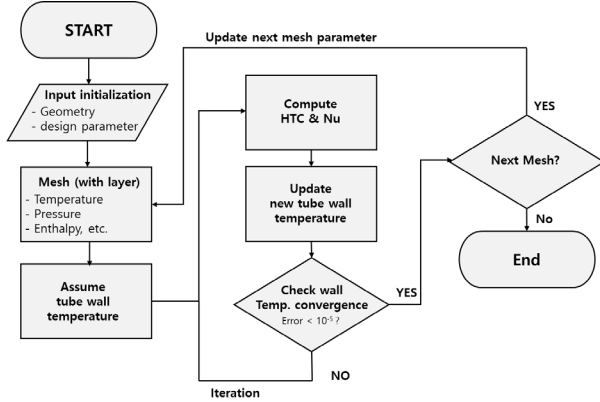


Fig. 2. Flow chart of KAIST-HCHXD.

For the design of a helium-helium intermediate heat exchanger (IHX), this study applies the Abadzc correlation for the shell side, as it provides generalized heat transfer equations based on data from multiple sources, covering an extended range of Reynolds numbers [5]. Since the tube side operates at high Reynolds numbers, this correlation is particularly relevant. However, Abadzc does not provide a friction factor correlation, though the shell-side pressure drop is expected to be insignificant in this design [2].

For the tube side, the Mori and Nakayama correlation is used to account for the effects of the helical tube geometry on heat transfer [5]. The applied correlations are detailed in Equations (1.1), (1.2), (1.3), (2), and (3), respectively.

$$Nu = 0.332 \cdot Re^{0.6} \cdot Pr^{0.36} \quad (1 \times 10^3 < Re < 2 \times 10^4) \quad (1.1)$$

$$Nu = 0.123 \cdot Re^{0.7} \cdot Pr^{0.36} \quad (2 \times 10^4 < Re < 2 \times 10^5) \quad (1.2)$$

$$Nu = 0.036 \cdot Re^{0.8} \cdot Pr^{0.36} \quad (2 \times 10^5 < Re < 9 \times 10^5) \quad (1.3)$$

$$Nu = \frac{Pr \cdot Re^{0.8} \left(\frac{d}{D}\right)^{0.1} \left[1 + \frac{0.098}{Re \left(\frac{d}{D}\right)^2}\right]}{26.2 \cdot Re^{0.666} - 0.074} \quad \text{for } Pr < 1 (\text{gases}) \quad (2)$$

$$f = \frac{0.305 \left[1 + \frac{0.112}{Re \left(\frac{d}{D}\right)^2}\right]^{0.2} \sqrt{d/D}}{4 \left[Re \left(\frac{d}{D}\right)^2\right]^{0.2}} \quad (3)$$

where,

d = tube diameter

D= coil diameter

On the primary side, the flow moves across the tube bundle. As the fluid enters the bundle, the flow area decreases due to the tube arrangement, causing an

increase in velocity. Therefore, the flow characteristics within the tube bundle are governed not by the average velocity but by the maximum velocity occurring within the bundle [6].

Accordingly, the Reynolds number is defined based on the maximum velocity and is given by Equation (4) [6]. The maximum velocity (V_{max}) can be calculated using Equation (5) [6].

$$Re_D = \frac{\rho V_{max} D}{\mu} \quad (4)$$

$$V_{max} = \frac{S_T}{S_T - D} V \quad (5)$$

where,

S_T = pitch

3. Results and discussion

The KAIST-HCHXD results are evaluated by comparing them with the IHX designs from General Atomics (GA) and AREVA. The primary and secondary side boundary conditions (temperature, pressure, and mass flow rate) were set identically across all three models to ensure a consistent basis for comparison.

Table 1 presents the major IHX design and performance comparisons between GA and AREVA. Effectiveness is calculated based on the given inlet and outlet temperature conditions, mass flow rates, and the specific heat capacity of helium. All other values are documented as referenced in the cited literature [3,4].

Table 1. Comparison of IHX design and performance between GA and AREVA [3,4].

Parameter	GA	AREVA
Heat load [MW _{th}]	178	290
Effectiveness [%]	70.9 %	84.5 %
ΔT_m [K]	185.6	75
$A_{\text{heat transfer}}$ [m ²]	2,740	3,567
$D_{\text{coil outer}}$ [m]	4.08	3.47
$L_{\text{tube height}}$ [m]	4.58	7.8

3.1 Design evaluation with GA IHX

Key geometric parameters such as tube OD, thickness, coil inner and outer diameter, number of coils, and pitch were identical inputs. However, coil height, elevation angle, and tube length were calculated as results, showing slight variations but maintaining overall consistency. Despite identical boundary conditions, minor differences were observed in temperatures, leading to slight variations in heat load. However, the differences are negligible. The secondary side pressure drop was evaluated, and while minor differences were observed, the overall results remained consistent across all models. Overall, KAIST-HCHXD produces results consistent with the previously reported IHX designs, as detailed in Table 2. The table distinguishes between input and output parameters, with the output section including the differences between the reference model and the KAIST-designed values for better comparison.

Table 2. Comparison of the KAIST-HCHXD results with GA and ANL design [3].

Input		GA	KAIST	Δ value
Primary side (shell)	T_{in} [°C]	900	900	-
	\dot{m} [kg/s]	81.8	81.8	-
	T_{out} [°C]	480	480	-
	P_{in} [MPa]	7.0	7.0	-
Secondary side (tube)	T_{in} [°C]	308	308	-
	\dot{m} [kg/s]	87.64	87.64	-
	T_{out} [°C]	700	700	-
	P_{in} [MPa]	7.1	7.1	-
Tube	OD [mm]	45	45	-
	T [mm]	5	5	-
	# tubes	550	550	-
	# coils	18	18	-
	$D_{inner\ coil}$ [mm]	1870	1870	-
	$D_{outer\ coil}$ [mm]	4080	4080	-
	Pitch [mm]	65	65	-
Output		GA	KAIST	Δ value
Heat load [MW _{th}]		178	178.8	+0.8
Primary side(shell)	T_{in} [°C]	900	901.3	+ 1.3
	ΔP [MPa]	0.004	-	-
Secondary side(tube)	T_{out} [°C]	700	701.3	+ 1.3
	ΔP [MPa]	0.079	0.035	- 0.044
Tube	Length [m]	22.05	21.42	- 0.63
Coil bundle	Angle	12	12.02	+ 0.02
	Height [m]	4.58	4.45	- 0.13

Figures 3 and 4 show the heat transfer coefficient and temperature profiles along the tube length based on the KAIST-HCHXD results for the GA design. In Fig. 3, the secondary side has a higher heat transfer coefficient (~2500 W/m²·K) measured across different layers, while the primary side is lower, around 1200-1300 W/m²·K. Fig. 4 illustrates the temperature profiles for the primary fluid, tube outer and inner walls, and the secondary fluid, showing an increase in temperature along the length.

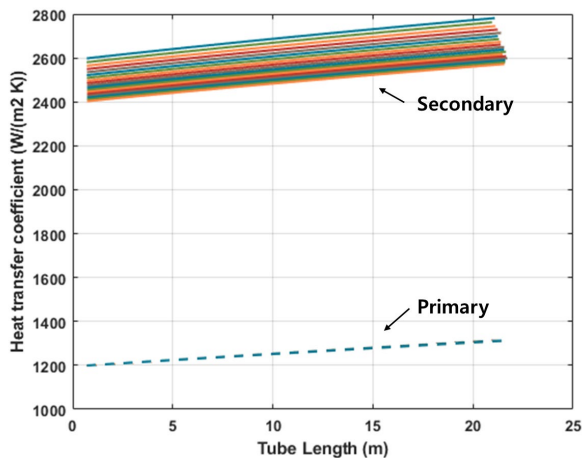


Fig. 3. Heat transfer coefficient of GA IHX using KAIST-HCHXD

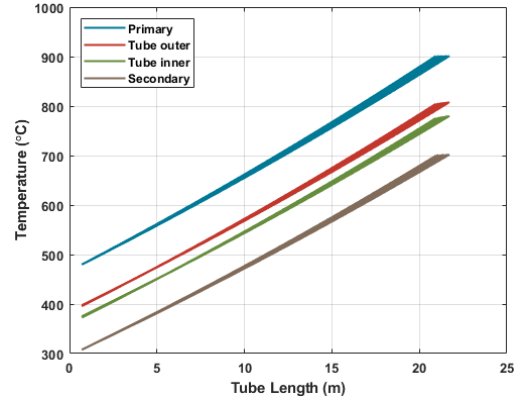


Fig. 4. Temperature profile of GA IHX using KAIST-HCHXD

3.2 Design evaluation with AREVA IHX

The AREVA model design shows slightly greater differences compared to the GA model, as seen in Table 3. Due to the lack of disclosed information, pitch and the number of coils were estimated, leading to slight differences in the input data compared to AREVA. In the KAIST model, the total number of tubes is 79 more than in the AREVA design, as this adjustment was made to maintain a coil bundle angle similar to that of AREVA. ANL also followed a similar approach in their estimation process [2].

Table 3. Comparison of the KAIST-HCHXD results with AREVA and ANL design [4].

Input		AREVA	KAIST	Δ value
Primary side (shell)	T_{in} [°C]	900	900	
	\dot{m} [kg/s]	136	136	
	T_{out} [°C]	490	490	
	P_{in} [MPa]	5.0	5.0	
Secondary side (tube)	T_{in} [°C]	415	415	
	\dot{m} [kg/s]	136	136	
	T_{out} [°C]	825	825	
	P_{in} [MPa]	5.5	5.5	
Tube	OD [mm]	21	21	
	T [mm]	2.2	2.2	
	# tubes	2966	3045	+ 79
	# coils	-	29	Inferred
	$D_{inner\ coil}$ [mm]	1500	1500	
	$D_{outer\ coil}$ [mm]	3478	3478	
	Pitch [mm]	-	35.3	Inferred
Output		AREVA	KAIST	Δ value
Heat load [MW _{th}]		290	289.2	- 0.8
Primary side(shell)	T_{in} [°C]	900	899.6	- 0.4
	ΔP [MPa]	0.02	-	-
Secondary side(tube)	T_{out} [°C]	825	824.7	- 0.3
	ΔP [MPa]	0.2	0.188	-0.012
Tube	Length [m]	18.3	20.6	+ 2.3
Coil bundle	Angle	25.38	25.36	- 0.02
	Height [m]	7.8	8.8	+ 1

Figures 5 and 6 show the heat transfer coefficient and temperature profiles for the AREVA design. The secondary side has a higher heat transfer coefficient ($\sim 3400 \text{ W/m}^2\cdot\text{K}$), while the primary side ranges from 2000 to 2200 $\text{W/m}^2\cdot\text{K}$. The temperature profiles follow a similar trend as the previous figures.

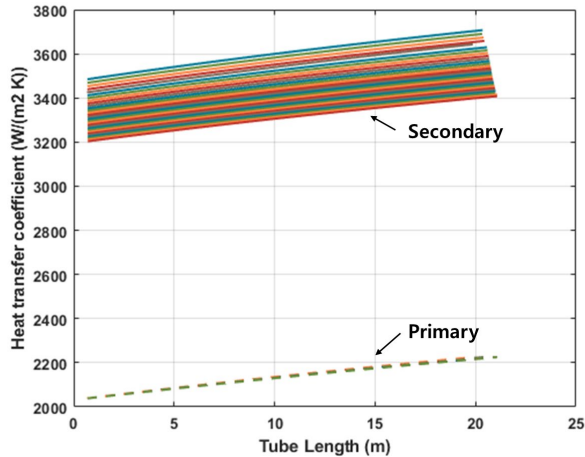


Fig. 5. Heat transfer coefficient of AREVA IHX using KAIST-HCHXD

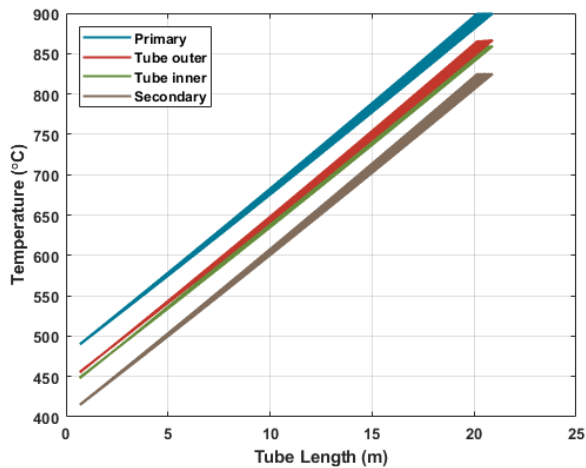


Fig. 6. Temperature profile of KAIST-HCHXD.

4. Conclusions and Further Works

This study evaluated the performance of the KAIST-developed one-dimensional Helical Coil Heat Exchanger Design Code (KAIST-HCHXD) by comparing its results with previous General Atomics (GA), AREVA. The results showed that KAIST-HCHXD produced comparable and reliable predictions for heat transfer, pressure drop, and temperature profiles, with small differences arising from variations in certain input parameters. The results demonstrated that KAIST-HCHXD can reasonably model helical coil heat exchangers, aligning closely with existing design data.

To further validate and improve the KAIST-HCHXD code, future work should include verification with other fluids, such as those used in AGR and LMFBR systems.

This will allow the model to be applied to a wider range of reactor types. Once validated, the code can be used to design helical coil heat exchangers with different fluid combinations, enhancing the design flexibility for future nuclear reactors.

ACKNOWLEDGEMENTS

This work was supported by the National Research Foundation of Korea (NRF) grant funded by the Korea government (MSIT)(No. : RS-2024-00436693).

REFERENCES

- [1] Gilli, P. V. *Review of problems governing the design optimization of heat exchangers in nuclear power plant*. No. IAEA--135. 1971.
- [2] S. Majumdar, A. Moiseyev, and K. Natesan. *Assessment of the Next Generation Nuclear Plant Intermediate Heat Exchanger Design* (ANL/EXT-08-32). Argonne National Laboratory. (2008)
- [3] Hanson, D. L. "Engineering Services for the Next Generation Nuclear Plant (NGNP) with Hydrogen Production." *General Atomics* 911117 (2008).
- [4] AREVA, NP. "NGNP with Hydrogen Production IHX and Secondary Heat Transport Loop Alternatives." (2008).
- [5] Smith, E. M., "Thermal Design of Heat Exchangers, A Numerical Approach: Direct Sizing and Stepwise Rating", John Wiley & Sons, Chichester, 1997.
- [6] Cengel, Yunus A., and Afshin Jahanshahi Ghajar. (*TEE-815*): *Heat and Mass Transfer: Fundamentals and Applications (Chap No. 15, 16 & 17 Includes)*. McGraw-Hill Education, 2020.